

Single-Ferroelectric Memcapacitor-Based Time-Domain Content-Addressable Memory for Highly Precise Distance Function Computation

Minjeong Ryu, Jae Seung Woo, Yeonwoo Kim, and Woo Young Choi

Abstract— Single ferroelectric memcapacitor-based time-domain (TD) content-addressable memory (CAM) is proposed and experimentally demonstrated for high reliability and density. The proposed TD CAM features the symmetric capacitance-voltage characteristics of a ferroelectric memcapacitor with a gated p-i-n diode structure. This CAM performs search operations based on the variable capacitance of cells. The propagation delay of the TD CAM output signal is linearly correlated with the Hamming distance (HD) between input and output vectors. The proposed TD CAM array exhibits exceptional reliability in HD computation and in-memory search tasks owing to this linearity, considerably outperforming the conventional nonlinear voltage-domain CAM.

Index Terms—ferroelectric memcapacitor, time-domain (TD) content-addressable memory (CAM), capacitive in-memory computing.

I. INTRODUCTION

CONTENT-ADDRESSABLE-MEMORY-BASED (CAM-based) in-memory nearest neighbor (NN) search is advancing applications in edge artificial intelligence (AI), including memory-augmented neural networks for one- or few-shot learning and hyperdimensional computing [1]–[5]. The key function of CAM in this type of associative search is the parallel computation of the Hamming distance (HD), which measures the degree of mismatch between a query vector and stored vectors. However, conventional voltage-domain (VD) CAMs suffer from a nonlinear relationship between the HD and voltage output, as the search operation relies on Ohm’s law and Kirchhoff’s laws [1]–[6]. Resistive HD computing schemes encounter comprehensive constraints in system-level performance, such as degraded accuracy, lower sensing margin, and inevitable area/power overhead of peripheral circuits arising from nonlinearity [6]–[10].

To overcome these problems, a time-domain (TD) CAM has been proposed, encoding bits based on cell capacitance rather than conductance [6]–[10]. By adjusting the variable capacitance instead of the driving current, the HD computation results can be linearly converted into the time delay of the

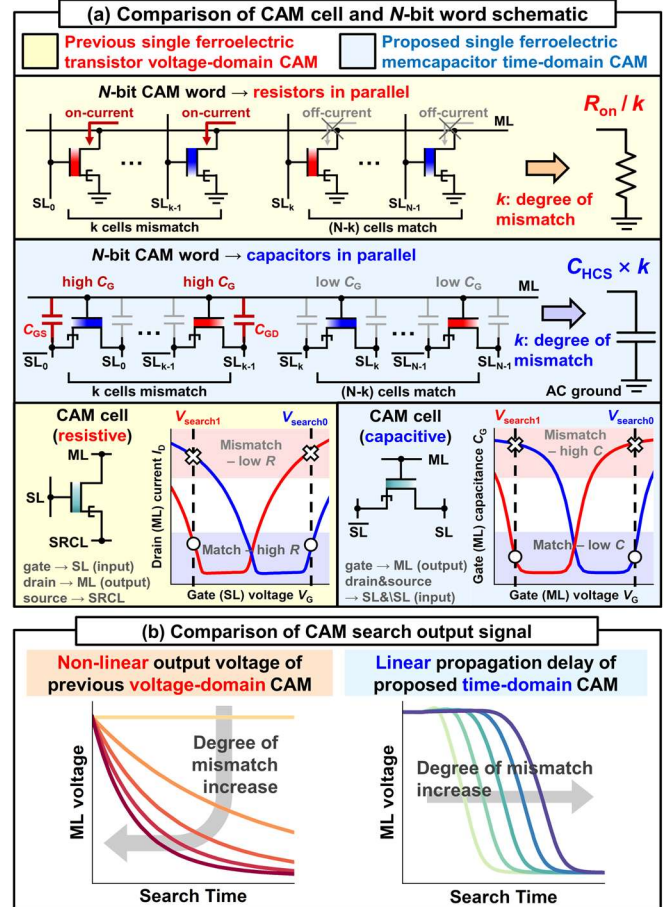


Fig. 1. Comparison of the previous one-transistor VD CAM with the proposed one-memcapacitor TD CAM (a) in terms of operation mechanism and (b) search output signal.

output signal [6]–[8], [11]. In addition to the high precision of NN searches associated with linearity, capacitive computing is advantageous because of its remarkable energy efficiency due to its negligible static current and high resilience to device variations [6], [13]–[20]. Moreover, TD CAM has compact peripheral circuitry owing to its digital compatibility [6]–[12].

This study proposes a novel TD CAM based on a single ferroelectric memcapacitor with symmetric capacitance–

This work was supported in part by Samsung Research Funding & Incubation Center of Samsung Electronics under Project Number SRFC-TA2103-01 and in part by the NRF of Korea funded by the MSIT under Grant RS-2024-00402495, NRF-2022M3I7A1078544 (PIM Semiconductor Technology Development Program). (Corresponding

Author: Woo Young Choi.)

M. Ryu, J. S. Woo, Y. Kim, and W. Y. Choi are with the Department of Electrical and Computer Engineering and the Inter-university Semiconductor Research Center (ISRC), Seoul National University, Seoul 08826, Republic of Korea (e-mail: wooyoung@snu.ac.kr).

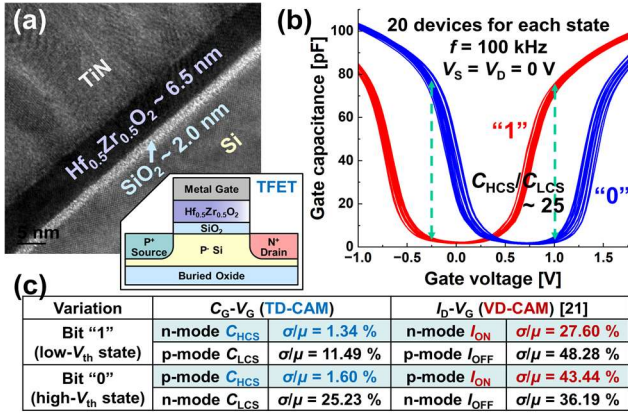


Fig. 2. (a) Cross-sectional TEM image of the gate stack of the fabricated ferroelectric memcapacitor and its schematic with the TFET structure. (b) Measured C - V curves (gate area = 10000 μm^2) and (c) extracted coefficient of variation from device characteristics. Two shaded rows C_{HCS} and I_{ON} plays the main role in driving the CAM response.

TABLE I

WRITE AND SEARCH BIAS SCHEMES FOR THE PROPOSED TD CAM

Operation	Write		Search	
	Bit "1"	Bit "0"	Bit "1"	Bit "0"
^a Node and pulse value	$V_{ML} = 6.5\text{V}$, 500 ns	$V_{ML} = -6.5\text{V}$, 500 ns	$V_{SL} = V_{ISL}$ = 0.3 V	$V_{SL} = V_{ISL}$ = -1.0 V

^aNodes not indicated are all grounded during specified operation.

voltage (C - V) characteristics, as illustrated in Fig. 1a. In this configuration, the high- (C_{HCS}) and low-capacitance states (C_{LCS}) of the ferroelectric memcapacitor indicate the mismatch and match states, respectively. This is analogous to previous VD CAM designs based on single ferroelectric transistors with ambipolar current-voltage (I - V) characteristics, where the on-current (I_{ON}) and off-current (I_{OFF}) of the cell correspond to the mismatch and match states, respectively [21], [22]. The proposed scheme addresses the nonlinearity problem of the previous single-transistor VD CAM, as depicted in Fig. 1b. The propagation delay of the proposed TD CAM output is modulated linearly with the HDs as the computed results are transformed into the summation of the capacitors in parallel.

II. RESULTS AND DISCUSSION

A. Ferroelectric Memcapacitor Cell Characteristics

The ferroelectric memcapacitor in the TD CAM cell is based on the structure of p-i-n tunnel field-effect transistors (TFETs), as shown in the inset of Fig. 2a. The TD CAM cell configuration is illustrated in Fig. 1a, where the gate, drain, and source of the device are connected to the match line (ML), search line (SL), and search line bar (SL), respectively. The cross-sectional view in Fig. 2a illustrates the metal-ferroelectric-insulator-semiconductor (MFIS) gate stack of a device fabricated using a complementary metal oxide semiconductor (CMOS) gate-first process [21], [23]. Fig. 2b presents the measured symmetric C - V characteristics, wherein a high gate-to-source capacitance C_{GS} (p-type inversion), low gate capacitance (depletion), and high gate-to-drain capacitance C_{GD} (n-type inversion) appear in sequence [14], [24], [25]. This completely differs from the asymmetric nature of MOSFET C - V curves [16]–[20]. Additionally, as the C_{LCS} is determined by silicon depletion, our proposed memcapacitor offers a greater dynamic range and sensing margin compared to metal-ferroelectric-metal-based

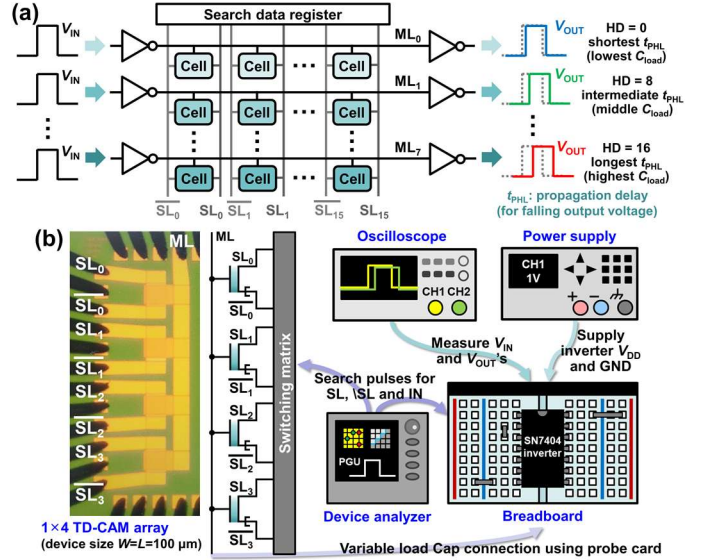


Fig. 3. (a) Design of the proposed TD CAM based on single ferroelectric memcapacitor. (b) Measurement environment of TD CAM search operation. The optical microscope image on the left is the top view of the fabricated 1 \times 4 TD CAM array tipped with multi-pin probe card.

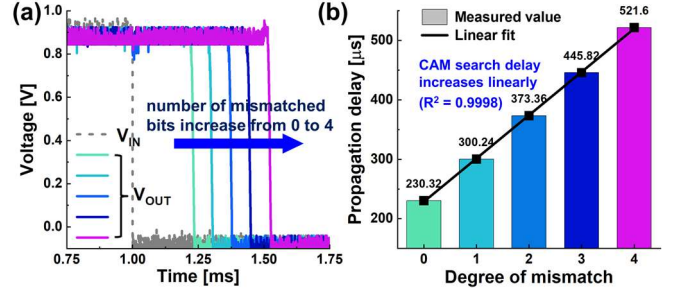


Fig. 4. (a) Measured transient waveforms of the proposed single TD CAM. (b) Measured TD CAM search delay which is linearly proportional to HD for the accurate evaluation of degree of mismatch.

(MFM-based) schemes [15]–[18].

Fig. 2c evaluates the variations in the measured capacitance and current [21]. The TD CAM cell exhibits less variation compared to the VD CAM cell, which leads to enhanced search reliability. The TFET I - V curves are sensitive to variations because their currents depend on the narrow tunneling region around the source and drain junctions. In contrast, the C - V properties are involved in the entire channel region where the inversion layer is formed [26], [27]. Table I summarizes the ML, SL, and $\bar{S}L$ voltages (V_{ML} 's, V_{SL} 's, and $V_{\bar{S}L}$'s) of the proposed TD CAM for the write and search operations. The cell capacitance states for bits "0" and "1" are updated by switching ferroelectric polarization via V_{ML} pulses. In the search operation, depending on the inputs V_{SL} and $V_{\bar{S}L}$, the matched and mismatched cells add C_{LCS} and C_{HCS} to the ML load capacitance, respectively.

B. TD CAM Measurement and Performance Prediction

To differentiate HDs for each ML based on the propagation delay, the proposed TD CAM incorporates single ferroelectric memcapacitor cells and two inverters per ML, as shown in Fig. 3a. The output of the first and the input of the second inverters are connected to the ML. The input of the first and the output of the second inverters are connected to the CAM input and output voltages (V_{IN} 's and V_{OUT} 's), respectively. In this

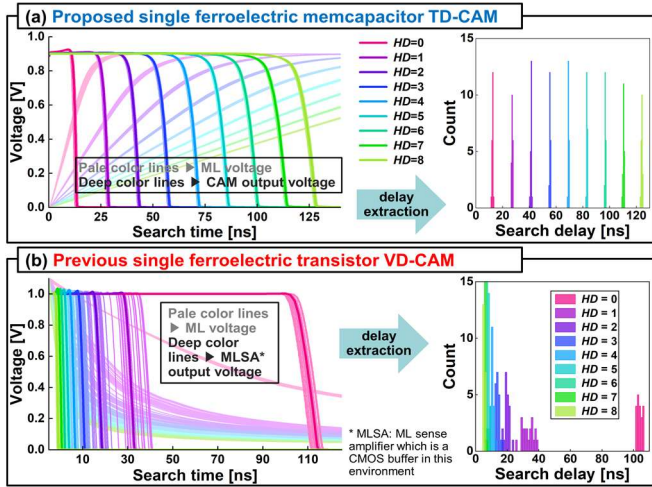


Fig. 5. Simulated transient response of V_{ML} 's and V_{OUT} 's during search operation (left) and extracted statistical distribution of search delay (right) evaluated for (a) proposed TD CAM and (b) previous VD CAM.

TABLE II

AREA COMPARISON OF THE PROPOSED AND THE PREVIOUS TD CAMS

TD-CAM cell structure	5T1C ^b	3T	1C
	[6], [7], [8]	[9], [10]	This work, [21]
Cell area ^a	304 F ² (~ 5.43 ×)	200 F ² (~ 3.57 ×)	56 F ² (1 ×)

^aF = half pitch. ^bT and C denote transistor and capacitor, respectively.

configuration, the tuned amount of ML load capacitance is directly proportional to the degree of mismatch. Consequently, the propagation delay from V_{IN} to V_{OUT} increases linearly in relation to the HD. Fig. 3b shows the measurement setup where the ML of the fabricated 1×4 TD CAM array is tied to inverters, and the Keysight B1500A semiconductor device analyzer and E5250A switching matrix supply signals.

Fig. 4 plots the measured search operation results of the proposed TD CAM. A linear correlation between the high-to-low propagation delay and the HD is experimentally verified. To evaluate search performance in larger arrays, Fig. 5 illustrates the SPICE Monte Carlo simulation results for the transient responses of 16-bit TD and VD CAM words [28]. The calibrated compact device model described in our previous works was applied by incorporating the variation parameters in Fig. 2c [21], [29]. The proposed TD CAM demonstrates higher reliability compared to the previous VD CAM for identifying HDs from 0 to 8 in 16-bit CAM words, assuming both utilize time-to-digital converters with equivalent resolution limits. The TD CAM achieves highly linear HD computing, offering narrower search delay distributions and improved sensing margins. In contrast, VD CAM suffers from nonlinear behavior and vulnerability to device variations, compromising the NN search accuracy.

Table II indicates that the proposed TD CAM achieves the highest integration density among existing ferroelectric TD CAMs [6]-[10]. Previous TD CAMs based on 5T1C and 3T architectures utilize ferroelectric memories as transistors rather than capacitors, requiring additional external capacitors or inverters per cell to separate each delay unit for linear TD operation. This requirement increases the cell size. In contrast, our proposed TD CAM employs ferroelectric memcapacitors as variable-capacitance load cells, optimizing area efficiency.

III. SUMMARY

A novel, high-density, and accurate TD CAM based on a single ferroelectric memcapacitor with symmetric C - V curves has been proposed. The proposed TD CAM demonstrates linear HD computation through modulation of the propagation delay. The proposed TD CAM outperforms previous single-transistor VD CAMs in terms of linearity and resilience to variation, achieving enhanced NN search accuracy and sensing margin. Moreover, the TD CAM offers superior energy efficiency and digital circuit compatibility. Furthermore, the proposed TD CAM achieves superior area efficiency compared to previous ferroelectric TD CAMs. Consequently, the proposed TD CAM is positioned as a promising solution for the performance and density limitations of the existing CAMs in on-device approximate search applications.

REFERENCES

- [1] K. Ni, X. Yin, A. F. Laguna, S. Joshi, S. Dünkel, M. Trentzsch, J. Müller, S. Beyer, M. Niemier, X. S. Hu, and S. Datta, “Ferroelectric ternary content-addressable memory for one-shot learning,” *Nat. Electron.*, vol. 2, no. 11, pp. 521–529, 2019, doi: 10.1038/s41928-019-0321-3.
- [2] S. Dutta, A. Khanna, H. Ye, M. M. Sharifi, A. Kazemi, M. San Jose, K. A. Aabrar, J. G. Mir, M. Niemier, X. S. Hu, and S. Datta, “Lifelong learning with monolithic 3D ferroelectric ternary content-addressable memory,” in *IEDM Tech. Dig.*, Dec. 2021, pp. 374–377, doi: 10.1109/IEDM19574.2021.9720495.
- [3] A. Kazemi, M. M. Sharifi, A. F. Laguna, F. Müller, X. Yin, T. Kämpfe, M. Niemier, and X. S. Hu, “FeFET multi-bit content-addressable memories for in-memory nearest neighbor search,” *IEEE Trans. Comput.*, vol. 71, no. 10, pp. 2565–2576, Oct. 2022, doi: 10.1109/TC.2021.3136576.
- [4] J. S. Lee, J. Yoon, and W. Y. Choi, “In-memory nearest neighbor search with nanoelectromechanical ternary content-addressable memory,” *IEEE Electron Device Lett.*, vol. 43, no. 1, pp. 154–157, Jan. 2022, doi: 10.1109/LED.2021.3131184.
- [5] Y. Li, J. Tang, B. Gao, J. Yao, A. Fan, B. Yan, Y. Yang, Y. Xi, Y. Li, J. Li, W. Sun, Y. Du, Z. Liu, Q. Zhang, S. Qiu, Q. Li, H. Qian, and H. Wu, “Monolithic three-dimensional integration of RRAM-based hybrid memory architecture for one-shot learning,” *Nat. Commun.*, vol. 14, no. 1, pp. 7140–7023, Nov. 2023, doi: 10.1038/s41467-023-42981-1.
- [6] K. Ni, Y. Xiao, S. Deng, V. Narayanan, “Computational associative memory powered by ferroelectric memory,” in *Proc. Device Res. Conf. (DRC)*, Jun. 2023, pp. 1–2, doi: 10.1109/drc58590.2023.10187008.
- [7] Q. Huang, H. E. Barkam, Z. Yang, J. Yang, T. Kämpfe, K. Ni, G. L. Zhang, B. Li, U. Schlichtmann, M. Imani, C. Zhuo, X. Yin, “A FeFET-based time-domain associative memory for multi-bit similarity computation,” in *Proc. Design, Autom. Test Eur. Conf. Exhib. (DATE)*, 2024, doi: 10.23919/DAT58400.2024.10546522.
- [8] X. Yin, Q. Huang, H. E. Barkam, F. Muller, S. Deng, A. Vardar, S. De, Z. Jiang, M. Imani, U. Schlichtmann, X. S. Hu, C. Zhuo, T. Kämpfe, and K. Ni, “A homogeneous FeFET-based time-domain compute-in-memory fabric for matrix-vector multiplication and associative search,” *IEEE Trans. Comput.-Aided Des. Integr. Circuits Syst.*, to be published, 2024, doi: 10.1109/TCAD.2024.3492994.
- [9] W. Xu, Z. Fu, K. Wang, C. Su, J. Luo, Z. Chen, Q. Huang, and R. Huang, “A novel ferroelectric tunnel FET-based time-domain content addressable memory with high distance-metric linearity and energy efficiency for edge machine learning,” *2023 Silicon Nanoelectronics Workshop (SNW)*, Jun. 2023, doi: 10.23919/SNW57900.2023.10183946.
- [10] J. Luo, W. Xu, Y. Du, B. Fu, J. Song, Z. Fu, M. Yang, Y. Li, L. Ye, Q. Huang, and R. Huang, “Energy- and area-efficient Fe-FinFET-based time-domain mixed-signal computing in memory for edge machine learning,” in *IEDM Tech. Dig.*, pp. 438–441, Dec. 2021, doi: 10.1109/IEDM19574.2021.9720548.
- [11] J. Song, Y. Wang, M. Guo, X. Ji, K. Cheng, Y. Hu, X. Tang, R. Wang, and R. Huang, “TD-SRAM: time-domain-based in-memory computing macro for binary neural networks,” *IEEE Trans. Circuits Syst. I, Reg. Papers*, 2021, pp. 3377–3387.
- [12] M. Bavandpour, M. R. Mahmoodi, and D. B. Strukov, “Energy-efficient time-domain vector-by-matrix multiplier for neurocomputing and beyond,” *IEEE Trans. Circuits Syst. II, Express Briefs*, vol. 66, no. 9, pp. 1512–1516, Sep. 2019, doi: 10.1109/TCSII.2019.2891688.
- [13] X. Ma, H. Zhong, N. Xiu, Y. Chen, G. Yin, V. Narayanan, Y. Liu, K. Ni, H. Yang, and X. Li, “CapCAM: A multilevel capacitive content addressable memory for high-accuracy and high-scalability search and compute applications,” *IEEE Trans. Very Large Scale Integr. (VLSI) Syst.*, vol. 30, no. 11, pp. 1770–1782, Nov. 2022, doi: 10.1109/TVLSI.2022.3198492.
- [14] K.-U. Demasius, A. Kirschen, and S. Parkin, “Energy-efficient memcapacitor devices for neuromorphic computing,” *Nat. Electron.*, vol. 4, no. 10, Oct. 2021, pp. 748–756, doi: 10.1038/s41928-021-00649-y.
- [15] W. Xu, Z. Fu, K. Wang, C. Su, J. Luo, Z. Chen, Q. Huang, and R. Huang, “A novel small-signal ferroelectric capacitance-based content addressable memory for area- and energy-efficient lifelong learning,” *IEEE Electron Device Lett.*, vol. 45, no. 1, pp. 24–27, Jan. 2024, doi: 10.1109/LED.2023.3333849.
- [16] Z. Zhou, J. Leming, J. Zhou, Z. Zheng, Y. Chen, K. Han, Y. Kang, and X. Gong, “Experimental demonstration of an inversion-type ferroelectric capacitive memory and its 1 kbit crossbar array featuring high C_{HCS}/C_{LCS} , fast speed, and long retention,” in *Proc. IEEE Symp. VLSI Technol. Circuits (VLSI Technol. Circuits)*, Jun. 2022, pp. 357–358, doi: 10.1109/VLSITechnologyandCir46769.2022.9830291.
- [17] S. Yu, Y. -C. Luo, T. -H. Kim and O. Phadke, “Nonvolatile capacitive synapse: device candidates for charge domain compute-in-memory,” *IEEE Electron Devices Magazine*, vol. 1, no. 2, pp. 23–32, Sep. 2023, doi: 10.1109/MED.2023.3293060.
- [18] E. Yu, G. Kumar K, U. Saxena, and K. Roy, “Ferroelectric capacitors and field-effect transistors as in-memory computing elements for machine learning workloads,” *Sci. Rep.*, vol. 14, no. 4, pp. 9426–9440, 2024, doi: 10.1038/s41598-024-59298-8.
- [19] T.-H. Kim, O. Phadke, Y.-C. Luo, H. Mulaosmanovic, J. Mueller, S. Duenkel, S. Beyer, A. I. Khan, S. Datta, and S. Yu, “Tunable non-volatile gate-to-source/drain capacitance of FeFET for capacitive synapse,” *IEEE Electron Device Lett.*, vol. 44, no. 10, pp. 1628–1631, Oct. 2023, doi: 10.1109/LED.2023.3311344.
- [20] Z. Zhou, H. Zhong, L. Jiao, Z. Zheng, H. Yang, T. Kämpfe, K. Ni, X. Li, and X. Gong, “First demonstration of charge-domain content addressable memory based on ferroelectric capacitive memory for reliable and low-power one-shot learning,” *Research Square preprint*, 2024, doi: 10.21203/rs.3.rs-5029047/v1.
- [21] M. Ryu, J. S. Woo, C. L. Jung, and W. Y. Choi, “One-transistor ternary content-addressable memory based on localized ferroelectric switching for massive and accurate routing,” *IEEE Electron Device Lett.*, vol. 45, no. 2, pp. 144–147, Feb. 2024, doi: 10.1109/LED.2023.3345412.
- [22] J. Luo, W. Xu, B. Fu, Z. Yu, M. Yang, Y. Li, Q. Huang, and R. Huang, “A novel ambipolar ferroelectric tunnel FinFET based content addressable memory with ultra-low hardware cost and high energy efficiency for machine learning,” in *Proc. IEEE Symp. VLSI Technol. Circuits (VLSI Technol. Circuits)*, Jun. 2022, pp. 226–227, doi: 10.1109/VLSITechnologyandCir46769.2022.9830413.
- [23] J. S. Woo, C. L. Jung, K. R. Nam, and W. Y. Choi, “Logic-compatible charge-trapping tunnel field effect transistors for low-power, high-accuracy, and large-scale neuromorphic systems,” *Adv. Intell. Syst.*, vol. 5, no. 11, Art. no. 2300242, Nov. 2023, doi: 10.1002/aisy.202300242.
- [24] C. Navarro, M. Bawedin, F. Andrieu J. Cluzel, and S. Cristoloveanu, “Fully depleted SOI characterization by capacitance analysis of p-i-n gated diodes,” *IEEE Electron Device Lett.*, vol. 36, no. 1, pp. 5–7, Jan. 2015, doi: 10.1109/LED.2014.2368596.
- [25] J. Franco, A. Alian, A. Vandooren, A. S. Verhulst, D. Linten, N. Collaert, and A. Thean, “Intrinsic robustness of TFET subthreshold swing to interface and oxide traps: A comparative PBTI study of InGaAs TFETs and MOSFETs,” *IEEE Electron Device Lett.*, vol. 37, no. 8, Aug. 2016, pp. 1055–1058, doi: 10.1109/LED.2016.2584983.
- [26] K. M. Choi and W. Y. Choi, “Work-function variation effects of tunneling field-effect transistors (TFETs),” *IEEE Electron Device Lett.*, vol. 34, no. 8, pp. 942–944, Aug. 2013, doi: 10.1109/LED.2013.2264824.
- [27] W. Lee and W. Y. Choi, “Influence of inversion layer on tunneling field-effect transistors,” *IEEE Electron Device Lett.*, vol. 32, no. 9, pp. 1191–1193, Sep. 2011, doi: 10.1109/LED.2011.2159257.
- [28] *HSPICE User Guide: Simulation and Analysis, S-2021.09*, Synopsys, Mountain view, CA, USA, Jun. 2008.
- [29] M. Ryu and W. Y. Choi, “Surface stoichiometry dependence of ambipolar SiGe tunnel field-effect transistors and its effect on the transient performance improvement,” *J. Semicond. Technol. Sci.*, vol. 24, no. 1, pp. 1–6, Feb. 2024, doi: 10.5573/JSTS.2024.24.1.1.